Regulation of the murine preadipocytes differentiation by bitter taste receptor Tas2r108 and Tas2r126

Eisuke Kato,[a*] Shota Oshima,[b] Yusuke Adachi,[b] and Reitaro Imai[b]

[a] *Research Faculty of Agriculture, Hokkaido University, Sapporo, Japan;* [b] *Graduate School of Agriculture, Hokkaido University, Sapporo, Japan*

* Corresponding author

Eisuke Kato, e-mail: eikato@eis.hokudai.ac.jp

ORCID: 0000-0001-9322-8589

Abstract

Taste 2 receptors (T2Rs) are known as receptors for sensing bitterness, but their gene expressions are observed in various extraoral tissues. T2Rs in adipocytes have attracted attention because bitter compounds influence lipid accumulation. However, the role of T2Rs in adipocytes has not been extensively investigated. This study investigated the functions of *Tas2r108* and *Tas2r126* in preadipocyte differentiation. Overexpression of *Tas2r108* or *Tas2r126* inhibited the differentiation of 3T3-L1 cells and mouse primary preadipocytes. Similarly, knockdown of *Tas2r108* suppressed the differentiation of these cells. Consistent with the knockdown results, stimulation with T2R agonists during the differentiation of 3T3-L1 cells enhanced adipogenesis. Mechanistic analysis revealed that the suppressed differentiation by T2R overexpression involves the downregulation of *Cebpb*, while T2R knockdown involves the upregulation of *Nr4a2* and *Nr4a3* and downregulation of *Egr2*. Analysis with T2R agonists revealed that T2Rs in preadipocytes couple with inhibitory G-protein to downregulate intracellular cAMP concentrations, which works through ERK to enhance adipogenesis. These results demonstrate the regulation of adipocyte differentiation by T2Rs and suggest that bitter compounds enhance adipogenesis via T2Rs.

Keywords

taste 2 receptor; bitter taste receptor; adipocyte; adipogenesis; obesity; Tas2r108; Tas2r126

Introduction

Taste 2 receptor (T2R) is a G-protein coupled receptor (GPCR) that is also known as a bitter taste receptor. The common role of T2Rs is to sense bitter taste; however, their gene expressions are observed in various tissues. The general physiological role of T2Rs is to sense harmful compounds and induce defensive responses. Extra-orally expressed T2Rs also follow this physiological role, stimulating the secretion of gastric acid to enhance the decomposition of harmful compounds in the stomach and inducing immune responses in airway and intestinal tuft cells through the detection of microbes and parasite-derived compounds [1].

In addition to their function as defensive receptors, T2Rs are suggested to control the metabolism of lipids and sugars and are associated with the risk of obesity and diabetes. From the analysis of T2Rs' genetic variations, the polymorphisms of *TAS2R4*, *TAS2R5*, and *TAS2R38* are found to associate with the risk of obesity [2-4], and the haplotype of T2R is associated with altered glucose and insulin homeostasis [5]. Oral administration of bitter taste receptor agonist KDT501 stimulates glucagon-like peptide 1 (GLP-1) through Tas2r108 to reduce fat mass and improve glucose homeostasis in diet induced obese mice [6]. In human trial, oral administration of bitter compound denatonium acetate (ARD-101) elevated the circulating level of GLP-1 [7].

The currently known metabolic functions of T2Rs are limited to the intestinal tract. However, T2Rs gene expression are observed in the white adipose tissue [8, 9], and bitter compounds like quinine, denatonium benzoate, and epigallocatechin gallate are shown to inhibit preadipocyte differentiation, suggesting that T2R may play a role in adipocytes [9, 10].

We previously reported that overexpression of *Tas2r108* or *Tas2r126* in 3T3-L1 cells inhibits their differentiation into mature adipocytes [11]. However, this overexpression study may not reflect the natural function of T2Rs in adipocytes. Furthermore, our previous results may have been influenced by the antibiotic selection period following transfection with the T2R expression plasmid vector. This period could lead to a decline in the differentiation capacity of 3T3-L1 cells as the number of passages increased. Therefore, to elucidate the function of T2R in adipocytes and obtain more reliable results, knockdown experiments and transfection methods that do not require a selection period should be employed.

In addition to the above technical issues, Ning et al. reported that quinine stimulation of Tas2r106

enhances the differentiation of mouse primary adipocytes [12]. Although the members of T2R differ from those in our previous report [11], an opposite role of T2R in adipocytes is shown. This also suggests the need for a more detailed study of Tas2r108 and Tas2r126 functions in adipocytes.

In this study, we constructed 3T3-L1 cells that overexpress or knocked-down *Tas2r108* or *Tas2r126* using adeno-associated viral vectors that do not require antibiotic selection. The constructed cells were used to investigate the role of T2Rs in adipogenesis and the cellular signaling pathways involved. The experiments were replicated in primary cultures of mouse-derived preadipocytes to confirm the results in normal cells.

Results

T2Rs control the adipogenesis of 3T3-L1 cells

AAV vectors of serotype 1 were used to overexpress or knockdown *Tas2r108* and *Tas2r126* in 3T3-L1 cells. Overexpression was confirmed by qPCR analysis and immunofluorescent staining, while knockdown was confirmed by qPCR analysis (Figure 1).

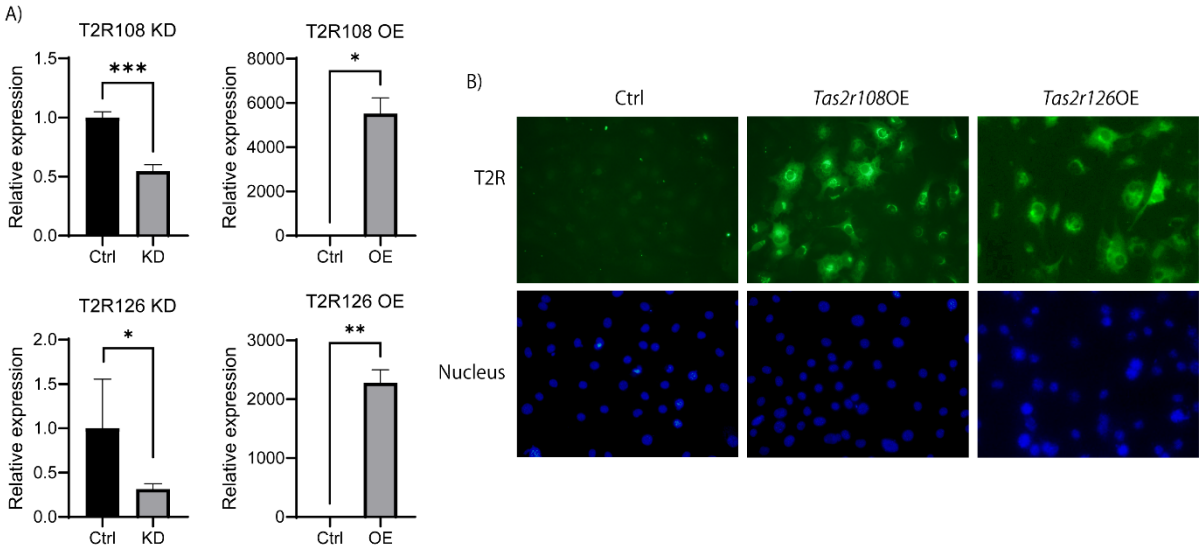

Figure 1. Overexpression (OE) and knockdown (KD) of *Tas2r108* and *Tas2r126* in 3T3-L1 cells. AAV vectors (1×10^{10} vg/well for OE and 5×10^{9} vg/well for KD) were added to 3T3-L1 cells seeded in 48 well plates, cultured for 5 days, and analyzed. A) qPCR analysis of T2Rs (N=3 for OE, N=5 for KD). B) Immunofluorescent staining of T2Rs using a PA-tag antibody (green) and DAPI (blue). *P<0.05, **P<0.01, ***P<0.001 vs Ctrl (t-test).

We then employed these AAV vectors in an overexpression experiment. AAV vectors for *Tas2r108* and *Tas2r126* overexpression were added to 3T3-L1 cells during differentiation, and their effects on adipogenesis were evaluated. Initially, general differentiation conditions for 3T3-L1 cells employing combinations of 3-isobutyl-1-methylxanthine (IBMX), dexamethasone, and insulin as differentiation inducers, followed by insulin as a differentiation enhancer, were employed. However, no differences in morphological characteristics or gene expression of *Pparg* and *Cebpa* were observed in the T2R overexpressed cells (Figure 2). Nevertheless, a slight decrease in lipid content was observed in the T2R overexpressed cells (Figure 2). Therefore, to visualize the effects of T2R overexpression more clearly, we conducted the experiment under milder differentiation conditions.

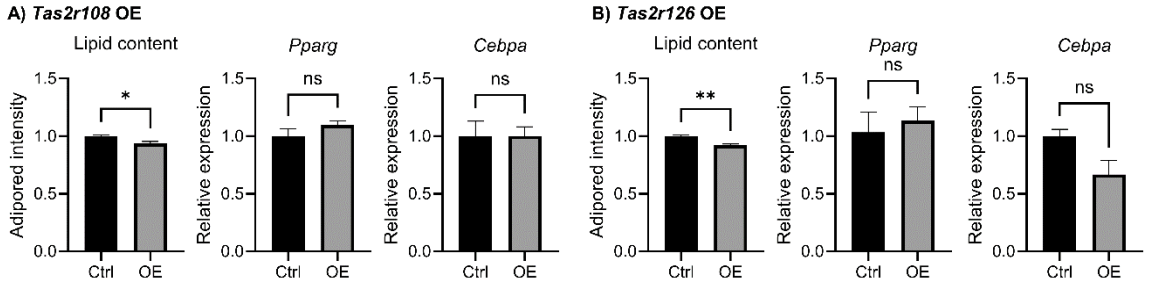

Figure 2. Effect of T2R overexpression (OE) on the differentiation of 3T3-L1 cells under general differentiation conditions. 3T3-L1 cells were seeded in 48-well plates and treated with an AAV vector (1×10^{10} vg/well) for 2 days of differentiation with IBMX, dexamethasone, and insulin. The cells were cultured in a growth medium containing insulin until day 6. Lipid content was measured using the AdipoRed™ assay reagent, and the expression of adipocyte marker genes was evaluated using qPCR. A) Tas2r108 OE (N=4), B) Tas2r126 OE (N=3). ns: no significance, *P<0.05, **P<0.01 vs Ctrl (t-test)

When *Tas2r108*- or *Tas2r126-overexpressed* cells were differentiated without a differentiation enhancer, morphological changes were apparently decreased, and lipid content decreased (Figure 3AB). Decreased expression of *Pparg* and *Cebpb*, together with lipid biosynthesis genes *Scd1* and *Gpat3*, in overexpressed cells showed a suppression of differentiation of 3T3-L1 cells through *Tas2r108* or *Tas2r126* overexpression (Figure 3C).

Tas2r108 knockdown cells were induced to differentiate, and the cells showed reduced morphological changes and lipid content (Figure 4AB). *Pparg* and *Cebpa* expression decreased, indicating the suppression of differentiation through the knockdown of *Tas2r108* (Figure 4C). In contrast, *Tas2r126* knockdown did not alter the morphological appearance or lipid content of 3T3-L1 cells, indicating no effect on the differentiation of preadipocytes (Figure 4AB).

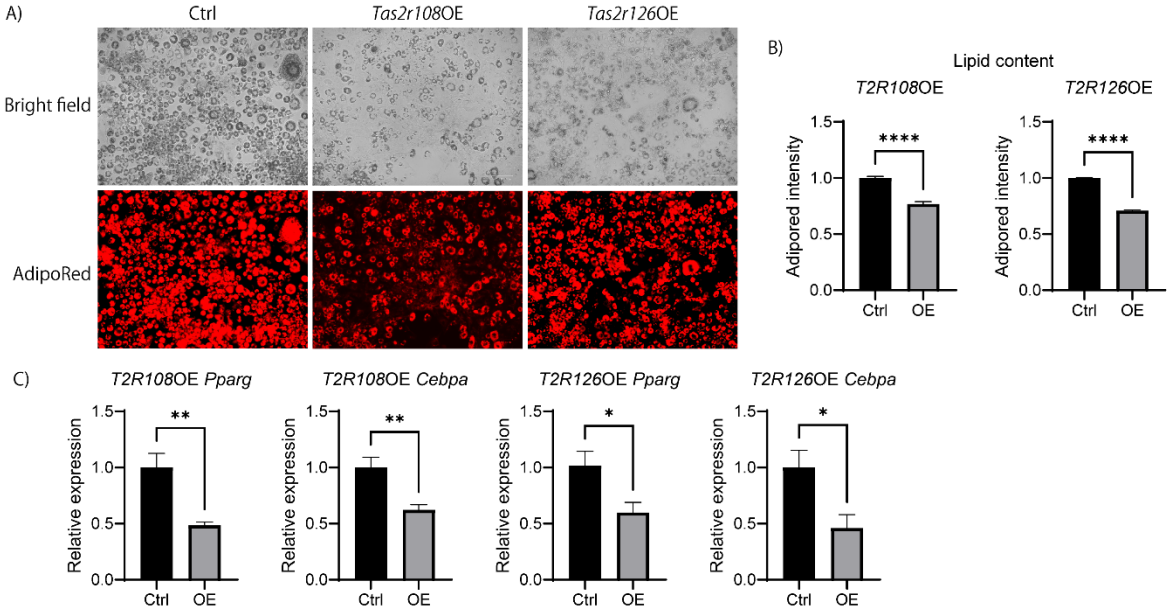

Figure 3. Overexpression (OE) of T2Rs suppressed the differentiation of 3T3-L1 cells. 3T3-L1 cells were seeded in 48 well plates and treated with an AAV vector (1×10^{10} vg/well) during 2 days of differentiation with IBMX, dexamethasone, and insulin. The cells were cultured in a growth medium until day 6. A) Cells stained with AdipoRed™ assay reagent. B) Lipid content evaluated from the fluorescence of the AdipoRed™ assay reagent (N=6). C) Expression of adipocyte marker genes (N=6). *P<0.05, **P<0.01, ****P<0.0001 vs Ctrl (t-test).

Since both knockdown and overexpression experiments resulted in the suppression of differentiation, 3T3-L1 cells were also treated with T2R agonists to evaluate the function of native T2R in adipocyte differentiation. When 3T3-L1 cells were differentiated under mild conditions, the addition of a T2R agonist elevated the lipid content in 3T3-L1 cells (Figure 4D) [13]. This enhancement was diminished in *Tas2r108* knockdown cells, demonstrating the contribution of Tas2r108 to the effect of the T2R agonist.

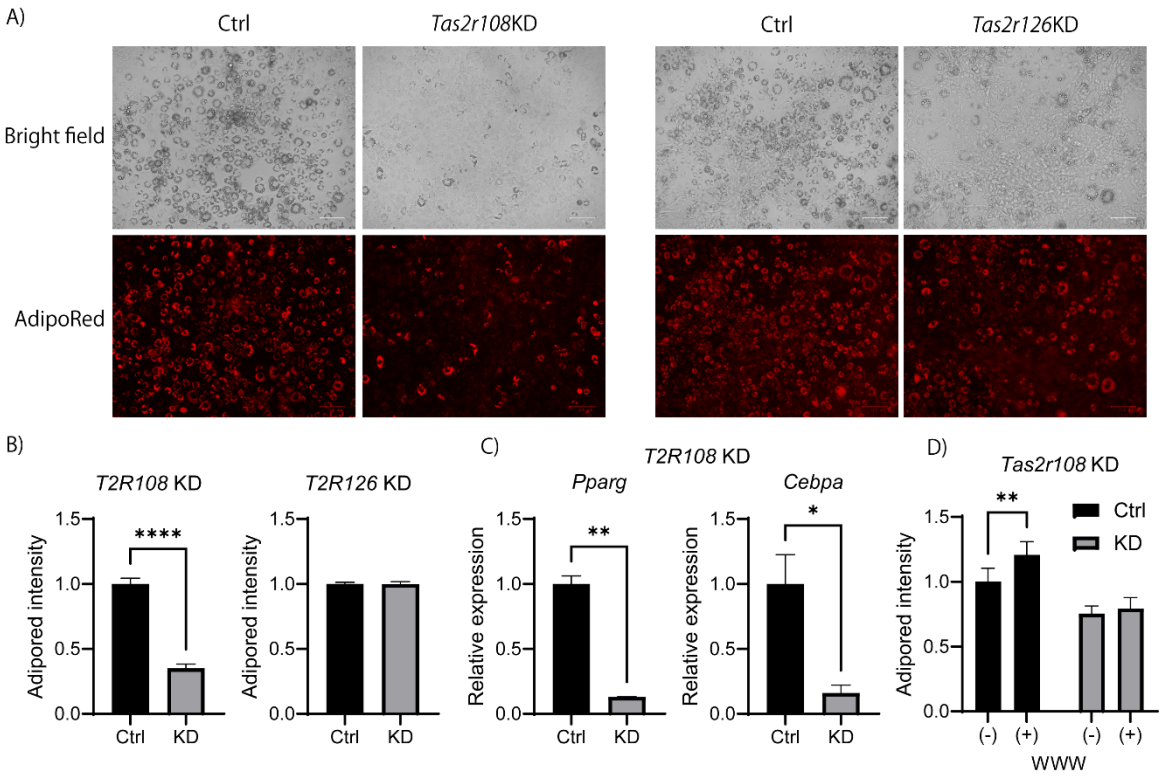

Figure 4. Altered differentiation in 3T3-L1 cells by *Tas2r108* knockdown (KD), but not by *Tas2r126* KD. 3T3-L1 cells were seeded in 48 well plates and treated with an AAV vector (5×10^9 vg/well) for 2 days of differentiation with IBMX, dexamethasone, and insulin. The cells were cultured in a growth medium until day 6. A) Cells stained with AdipoRed™ assay reagent. B) Lipid content evaluated from the fluorescence of the AdipoRed™ assay reagent (N=6). C) Expression of adipocyte marker genes (N=3). D) Lipid content of 3T3-L1 adipocytes treated with WWW (300 μM) with or without *Tas2r108* KD during differentiation and cultured until day 6 in the growth medium (N=6). ns: no significance, *P<0.05, **P<0.01, ****P<0.0001. t-test (B and C) and Tukey's multiple comparisons test (D).

Mechanistic analysis involved in the T2R mediated differentiation of preadipocytes

To elucidate the mechanisms involved in the regulation of preadipocyte differentiation via T2R, gene expression of transcription factors previously found to be associated with T2R signaling was examined in 3T3-L1 cells overexpressing or knocked-down T2R [11].

At 3 and 6 h after differentiation induction, no differences were observed in the expression of the transcription factors examined between T2R OE and KD cells compared to control cells (Supplementary Figure S1, S2). In *Tas2r108*-overexpressed cells, the expression levels of *Cebpb* and *Nr4a1* were decreased

144 at 48 h (Figure 5A). In *Tas2r126*-overexpressed cells, *Egr2* expression increased, whereas *Cebpb* showed a
145 decreasing trend (*P*=0.15) at 48 h (Figure 5A). In *Tas2r108*-knockdown cells, the expression of *Egr2* was
146 downregulated, whereas the expression of *Nr4a2* and *Nr4a3* were upregulated at 48 h (Figure 5B).
147 The expression of *Cebpb* and Nr4a family members is regulated via cAMP signaling [14, 15]. T2R
148 is a GPCR that modulates intracellular cAMP concentrations. Therefore, overexpression or knockdown of
149 T2R is expected to alter intracellular cAMP levels and modify the expression of *Cebpb* and *Nr4a* family.
150 Evaluation of intracellular cAMP concentrations confirmed decreased intracellular cAMP levels in *Tas2r108*
151 overexpressed cells, whereas increased cAMP levels were observed in *Tas2r108* knockdown cells (Figure
152 5C).
153 The change in intracellular cAMP concentration suggests that T2Rs are coupled with the inhibitory
154 Gα-protein ($G\alpha_i$). However, in co-immunoprecipitation analysis using PA-tagged Tas2r108 and anti-PA
155 antibody, $G\alpha_i$, which is expressed at relatively high levels in 3T3-L1 cells, was not detected (Supplementary
156 Figure S3-5). Therefore, we also co-incubated T2R ligands with the $G\alpha_i$ inhibitor pertussis toxin (PTX) and
157 showed that PTX diminished the effect of the T2R ligand in 3T3-L1 cells (Figure 5D). Additionally, the
158 contribution of Gβγ was eliminated because gallein, the inhibitor of Gβγ, had no effect on the activity of the
159 T2R ligand (Figure 5D). Finally, because Egr2 is regulated by ERK [16], we examined the effect of the
160 MEK1/2 inhibitor U0126 and found that the activity of the T2R ligand was diminished by inhibiting the
161 MEK-ERK cascade (Figure 5D).
162

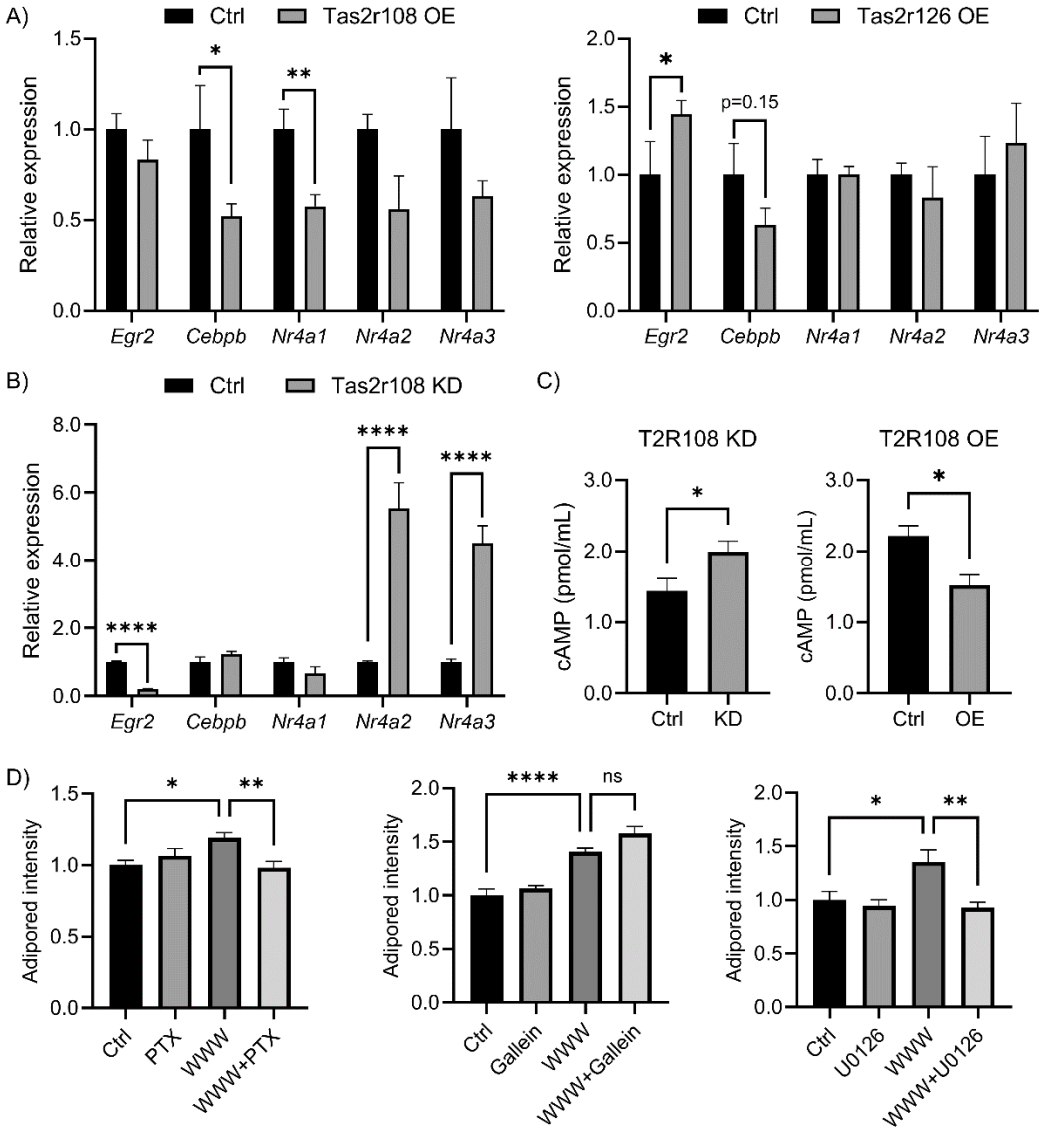

Figure 5. Analysis of pathways involved in T2R to control the differentiation of 3T3-L1 cells.

A,B) 3T3-L1 cells were seeded in 48 well plates and treated with an AAV vector (OE: 1×10^{10} vg/well, KD: 5×10^{9} vg/well) during 2 days of differentiation. Gene expression was assessed 48 h after differentiation induction (N=6). C) 3T3-L1 cells were seeded in 48-well plates and treated with an AAV vector for 3 days. The cells were stimulated with 0.1 mM forskolin and 0.5 mM IBMX for 1 h, and intracellular cAMP concentration was evaluated (N=4). D) Lipid content of 3T3-L1 adipocytes treated with 300 μM WWW with or without PTX (50 ng/mL), gallein (20 μM), or U0126 (20 μM) during differentiation and cultured until day 6 in growth medium (N=6). ns: no significance, *P<0.05, **P<0.01, ****P<0.0001. t-test (A-C) and Tukey's multiple comparisons test (D).

T2Rs control the differentiation in mouse primary preadipocytes

To confirm the above results in normal preadipocytes, we performed overexpression and knockdown experiments of *Tas2r108* and *Tas2r126* in mouse primary preadipocytes isolated from inguinal WAT.

Mouse primary preadipocytes were transfected with AAV, and overexpression of *Tas2r108* and *Tas2r126* was confirmed by the gene expression of T2R and immunofluorescent staining (Figure 6AB). Induction of differentiation in T2R overexpressed primary preadipocytes resulted in reduced morphological changes and lipid content (Figure 6CD). A reduction in the expression of *Pparg* and *Cebpa* was confirmed in the overexpressed cells, showing attenuated differentiation of the preadipocytes (Figure 6E).

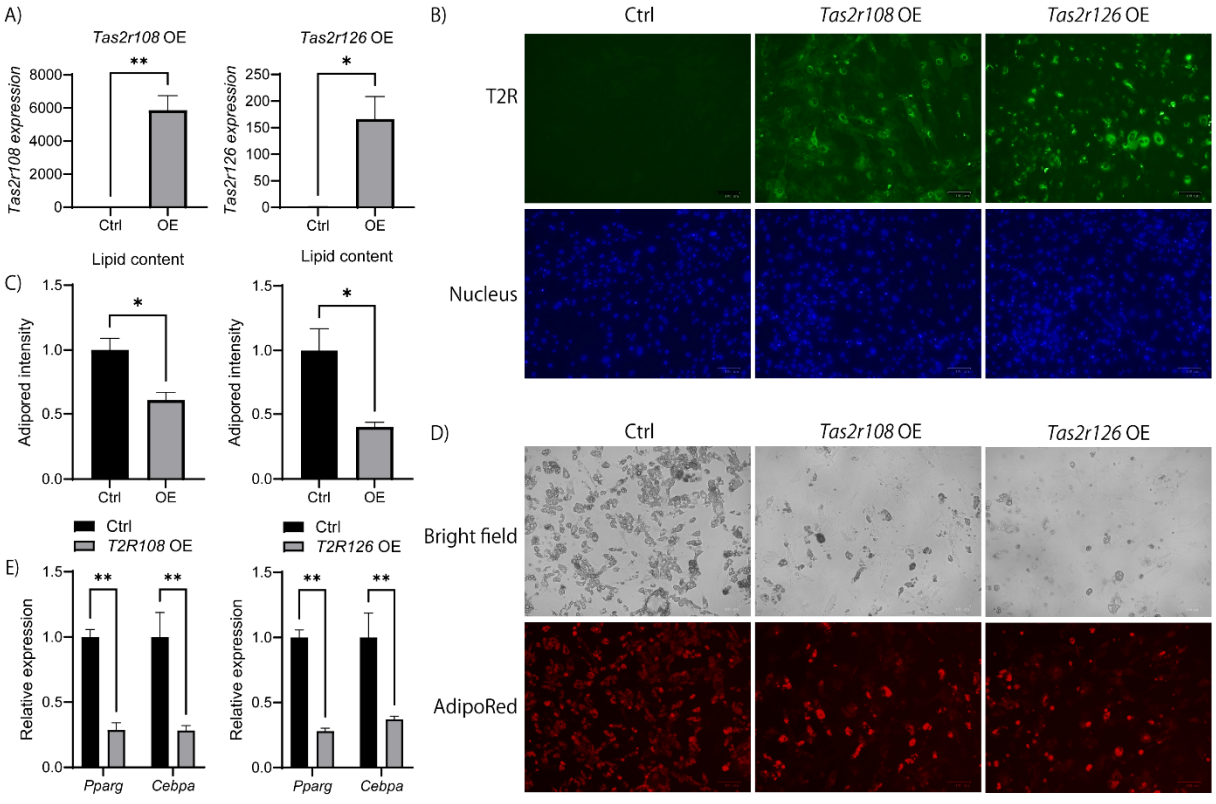

Figure 6. Overexpression of T2Rs suppresses the differentiation of mouse primary preadipocytes. Mouse primary preadipocytes were seeded in 48-well plates and treated with an AAV vector (1×10^{10} vg/well) for 6 days during differentiation. A) T2R gene expression on day 6 (N=3). B) Immunofluorescent staining of T2Rs on day 6 (N=3). C, D) Lipid content was visualized and measured using the AdipoRed™ assay reagent on day 11 (N=3). E) Expression of adipocyte marker genes on day 6 (N=3). *P<0.05, **P<0.01 (t-test).

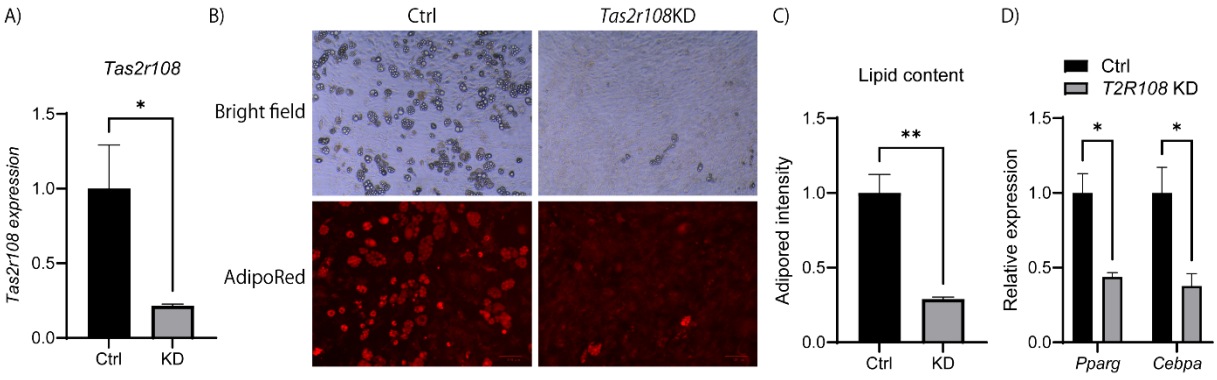

Figure 7. Knockdown of *Tas2r108* suppresses the differentiation of mouse primary preadipocytes. Mouse primary preadipocytes were seeded in 48-well plates and treated with an AAV vector (5×10^9 vg/well) for 3 days and then differentiated. A) *Tas2r108* expression (N=3). B) Lipid content was visualized and measured using the AdipoRed™ assay reagent on day 10. C) Lipid content on day 10 (N=3). D) Expression of adipocyte marker genes on day 10 (N=3). *P<0.05, **P<0.01 (t-test).

Discussion

Through the overexpression and knockdown of *Tas2r108* and *Tas2r126*, the current study revealed that the modulation of these T2Rs affects the capacity of preadipocyte differentiation. The use of an AAV vector provided high transfection efficacy and eliminated factors that could potentially affect the differentiation potential of preadipocytes, such as the toxicity of lipid-based transfection reagents and antibiotic selection processes, providing more reliable results to explore the function of T2Rs in preadipocyte differentiation.

Overexpression of T2Rs via AAV suppressed the differentiation of preadipocytes (Figure 3 and 6), which replicated the results of our previous overexpression experiment employing plasmids as vectors [11]. Additionally, we showed that knockdown of *Tas2r108* also suppressed the differentiation of preadipocytes (Figure 4 and 7). These results show that T2Rs, specifically Tas2r108, are involved in the regulation of preadipocyte differentiation. However, these results also raise the question of whether Tas2r108 plays a role in enhancing or suppressing preadipocyte differentiation. Considering that stimulation by the T2R agonist enhances lipid accumulation in 3T3-L1 cells (Figure 4D), as well as the findings by Ning et al. that quinine, an agonist of several T2Rs [17], promotes the differentiation of primary mouse preadipocytes [12], it is believed that the function of Tas2r108 in preadipocytes is to enhance their differentiation.

Mechanistic analysis revealed that Tas2r108 controls preadipocyte differentiation by modulating intracellular cAMP levels. In taste cells, activation of T2Rs transmits signals via Gβγ subunits, thereby increasing intracellular calcium concentrations to cause a bitter taste sensation [1]. However, T2Rs simultaneously reduce intracellular cAMP levels via the α-subunit $G\alpha_{gust}$ or other $G\alpha_i$ [18, 19]. cAMP signaling is important in the regulation of adipocyte differentiation, and intracellular cAMP levels were modulated in 3T3-L1 preadipocytes overexpressing or knocked-down *Tas2r108* (Figure 5C). While the $G\alpha_i$ inhibitor pertussis toxin suppressed the effect of the T2R agonist, no suppression was observed with the Gβγ inhibitor gallein (Figure 5D). Thus, the modulation of cAMP levels through the Gα subunit would be involved in the function of Tas2r108 in regulating preadipocyte differentiation. Notably, our previous analysis has shown that 3T3-L1 cells do not express $G\alpha_{gust}$ [8], therefore, $G\alpha_i$ would be contributing to this process, which remains to be clarified.

Although *Tas2r108* overexpression reduced and knockdown elevated intracellular cAMP levels, the resulting reduction in preadipocyte differentiation occurred through effects on different transcription factors. In cells overexpressing *Tas2r108 and Tas2r126*, a decrease in *Cebpb* expression (or a tendency) was observed (Figure 5A). C/EBPβ, the protein coded by *Cebpb*, is a crucial element in adipocyte differentiation, and its expression is controlled by cAMP [14]. C/EBPβ facilitates mitotic clonal expansion in the early stages and induces the expression of the two master adipogenic genes, *Pparg* and *Cebpa*, in the terminal stage of adipocyte differentiation [20]. Therefore, downregulation of *Cebpb* would be a major factor in suppressing differentiation in preadipocytes overexpressing *Tas2r108 and Tas2r126* (Figure 8).

In addition to *Cebpb*, downregulation of *Nr4a1* in *Tas2r108* overexpressed cells, and upregulation of *Egr2* in *Tas2r126* overexpressed cells were also detected (Figure 5A). The reduced expression of *Nr4a1* may also contribute to the suppression of preadipocyte differentiation, as knockdown of *Nr4a1* (synonym *Nur77*) delays adipogenesis in 3T3-L1 preadipocytes through a delayed mitotic clonal expansion process [21]. However, when T2Rs were overexpressed in preadipocytes and differentiation was subsequently induced, the effect on lipid content was minimal, and no effect was observed on the gene expression of *Pparg* and *Cebpa* (Supplementary Figure S6, 7). Clearer differences were observed when T2Rs were overexpressed concurrently with differentiation (Figure 3). Therefore, it is likely that the overexpression of T2R mainly functions through the downregulation of *Cebpb* during the terminal process of adipocyte differentiation,

241 rather than through the reduced expression of *Nr4a1* in the early process. Enhanced expression of *Egr2*
242 (*Krox20*) in *Tas2r126* overexpressed cells is not likely to contribute to the suppressed differentiation (Figure
243 5A), since Egr2 upregulates C/EBPβ expression to facilitate differentiation process [14].

244 In *Tas2r108* knockdown cells, intracellular cAMP concentration increased, but *Cebpb* expression was not
245 altered, and upregulation of *Nr4a2* and *Nr4a3* were observed (Figure 5B). Although elevated cAMP levels
246 are known to increase *Cebpb* expression, the increase in cAMP levels resulting from *Tas2r108* KD (1.4-fold)
247 was smaller than that induced by the differentiation cocktail (approximately 10-fold [22]). Therefore, it is
248 likely that the *Cebpb* expression levels were comparable to those in the control cells. This suggests that a
249 mechanism distinct from T2R overexpression is involved in the suppression of differentiation by *Tas2r108*
250 knockdown. *Nr4a2* and *Nr4a3* are transcription factors upregulated by cAMP stimulation, and their
251 overexpression inhibits adipogenesis [15]. Therefore, it is thought that knockdown of *Tas2r108* excessively
252 elevated intracellular cAMP levels to upregulate *Nr4a2* and *Nr4a3*, resulting in the suppression of
253 adipogenesis (Figure 8).

254 Based on the above findings and the results obtained from the use of T2R agonists and inhibitors (Figure
255 5D), the function of Tas2r108 in adipocytes can be summarized as follows. Tas2r108 modulates the
256 intracellular cAMP concentration via $G\alpha_i$, which results in the suppression of *Nr4a2* and *Nr4a3* expression.
257 Since Nr4a2 and Nr4a3 are reported to suppress ERK signaling [23, 24], suppression of *Nr4a2* and *Nr4a3*
258 expression results in the activation of ERK signaling, followed by upregulation of Egr2 to enhance
259 adipogenesis (Figure 8).

260 While the function of Tas2r108 was investigated as above, *Tas2r126* knockdown had no effect on the
261 differentiation of 3T3-L1 cells. This indicates that not all members of T2Rs regulate the differentiation of
262 preadipocytes or are functionally expressed in preadipocytes. The fact that knockdown of *Tas2r108*
263 completely eliminated the effect of T2R agonist may support this thought (Figure 4D), since WWW is also
264 the ligand of Tas2r126 [25].

265 Knockdown of *Tas2r108* reduced the differentiation potential of preadipocytes, even in the absence of
266 agonist addition. This also raises the question of what activates Tas2r108 under culture conditions. Tas2r108
267 recognizes a variety of compounds [17, 26], and TAS2R4, the human ortholog of Tas2r108, recognizes
268 tryptophan and peptides [13]. Therefore, one potential explanation is that Tas2r108 could be activated by

amino acids, peptides, or other compounds present in the culture medium. Further investigation is required to address this possibility.

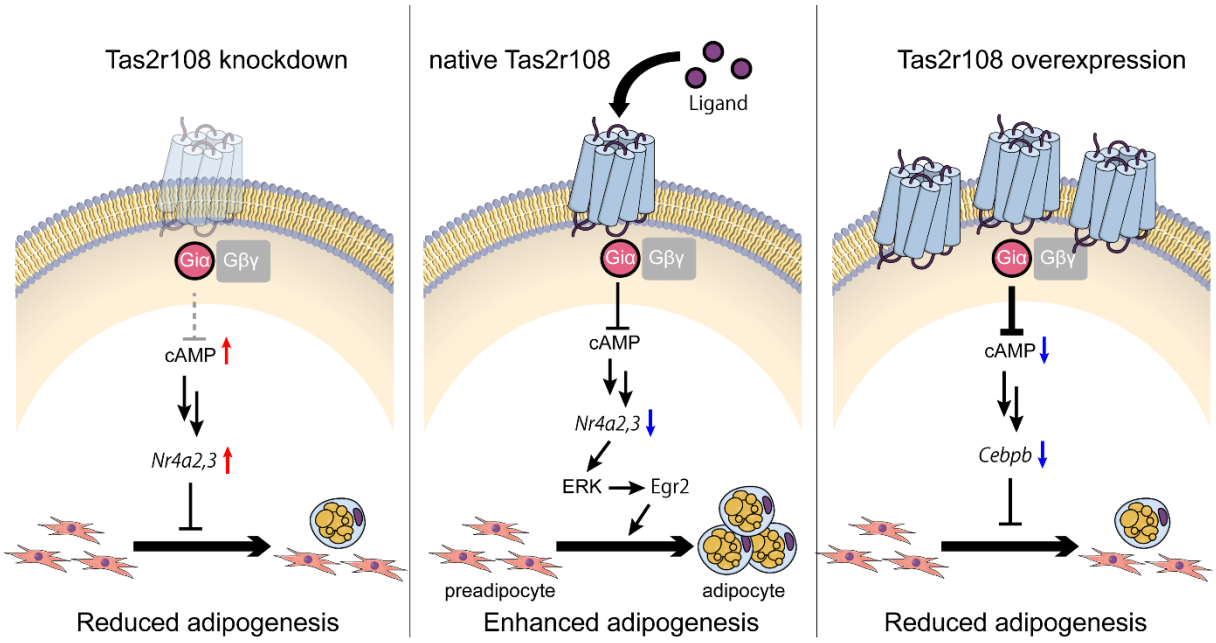

Figure 8. Regulation of adipogenesis by T2R. Activation of Tas2r108 modulates intracellular cAMP, which suppresses *Nr4a2* and *Nr4a3*, unlocking ERK signaling and upregulating Egr2 to enhance adipogenesis. Knockdown of Tas2r108 leads to excessive accumulation of cAMP, which in turn increases the expression of Nr4a2 and Nr4a3 and suppresses adipogenesis. Overexpression of Tas2r108 leads to an excessive decrease in cAMP, which in turn reduces *Cebpb* expression and suppresses adipogenesis.

The limitations of this study are that, although we have suggested that Nr4a2, Nr4a3, and Cebpb are involved in adipogenesis controlled by T2R, this was confirmed at the gene expression levels and not at the protein levels. Another limitation is the involvement of ERK. We inferred this involvement using the MEK inhibitor U0126; however, T2R-mediated ERK phosphorylation was not demonstrated. Furthermore, while we demonstrated the involvement of Gi using the Gi inhibitor PTX, we were unable to identify which of the many types of Gi is coupled to T2R and played a role in this process. These issues must be clarified in future studies.

In conclusion, in 3T3-L1 preadipocytes and mouse primary preadipocytes, Tas2r108 is involved in the

regulation of preadipocyte differentiation. Mechanistic investigations showed that Tas2r108 in preadipocytes couple with $G\alpha_i$ to modulate intracellular cAMP concentrations and downstream transcription factors *Nr4a2*, *Nr4a3*, and *Cebpb*, depending on their expression. Our research provides insights into the function of Tas2r108 in preadipocytes and their potential involvement in metabolic processes. Further studies, particularly those conducted in vivo, may shed light on the importance of Tas2r108 in the regulation of adipose tissue and its relationship with the effects of bitter compounds.

Materials and methods

Cell cultures

3T3-L1 cells (JCRB9014) were obtained from the Japanese Collection of Research Bioresources Cell Bank in Osaka, Japan. AAVpro® 293T cells were purchased from Takara Bio, Inc. (Shiga, Japan). Stromal vascular fraction cells prepared from the inguinal WAT tissue collected from 8-9 weeks old C57BL/6J Slc mice were used as the primary preadipocytes [27]. The animal experiments were approved (No. 24-0019) by the Institutional Animal Care and Use Committee of Hokkaido University, Japan. All operations were compliant with the National University Corporation Hokkaido University Regulations on Animal Experimentation. The cells were cultured at 37°C in a 10% carbon dioxide atmosphere in growth medium [Dulbecco's modified Eagle medium (DMEM) supplemented with 10% fetal bovine serum (FBS) and antibiotics (100 units/mL penicillin, 100 µg/mL streptomycin, and 50 µg/mL gentamicin)]. Pyruvic acid (1 mM) was added in the growth medium for AAVpro® 293T cells.

Preparation of adeno-associated virus (AAV) vectors

To construct the *Tas2r108* and *Tas2r126* overexpression plasmids, we amplified the gene fragments encoding *Tas2r108* (NM_020502.1) and *Tas2r126* (NM_207028.1), attached with the herpes simplex virus glycoprotein (HSV) epitope tag followed by a PA tag at the C-terminal region, using polymerase chain reaction (PCR) from a previously constructed plasmid vector [11]. pAAV-CAG-GFP (Addgene #37825) was treated with BamHI and EcoRI to prepare a linearized vector. We connected the insert fragments and the linearized vector using In-fusion® Snap Assembly Master Mix (Takara Bio Inc.) to prepare the plasmids. An empty vector for the control experiment was constructed from pAAV-CAG-GFP by removing the GFP

sequence.

To construct the *Tas2r108* knockdown plasmid, short hairpin RNA (shRNA) was designed against the target sequence (T2: CAGAAGATGCAGAGAAACAG, T4: GGTCAACAGTCGCAGAATTG), and the corresponding oligo DNA was purchased from Fasmac Co., Ltd. (Kanagawa, Japan). (Kanagawa, Japan). The GFP sequence was removed from the pX552-GFP plasmid (Addgene #107023), and the plasmid was treated with BspQ I to prepare a linearized vector. Oligo DNA and the linearized vector were ligated to prepare plasmids. A plasmid with a scrambled sequence of T2 and T4 target sequences (T2 scramble: GGACAAACGACTAGGAGAAA, T4 scramble: GACCATGCAAGGCGTAGTAT) was constructed in the same manner.

To construct the *Tas2r126* knockdown plasmid, the target sequence (T2: GGAGAAAGTTTACTGGGAAC, T4: CTAAGAATGCAGCACAATAC) was selected and inserted into the backbone of the miR-30 miRNA sequence [28]. The designed DNA fragment was purchased from GenScript (Tokyo, Japan). pAAV-CAG-GFP was linearized using BamHI and HindIII. The fragment DNA and linearized vector were ligated to prepare plasmids. A plasmid with a negative control target sequence (CCTAAGGTTAAGTCGCCCTCG) was constructed using the same method.

The constructed plasmids were transfected into AAVpro® 293T cells with pAAV-2/1 (Addgene #112862) and pHelper (Cell Biolabs Inc., CA, USA) using PEI Max (Polysciences, PA, USA). The next day, the medium was replaced with serum-free Dulbecco's modified Eagle's medium (DMEM), and the cells were cultured for an additional three days. Cells and medium were recovered and purified according to a previously described procedure to obtain AAV vectors for overexpression and knockdown [29]. Empty vectors for control in overexpression experiments and scrambled or negative control vectors for knockdown experiments were also prepared. AAV titers were measured by qPCR using primer pairs for the ITR sequence (forward, GGAACCCCTAGTGATGGAGTT; reverse, CGGCCTCAGTGAGCGA).

Immunofluorescent staining

3T3-L1 cells or mouse primary preadipocytes were seeded in 48 well plates at 5×10^4 cells/well, and AAV vectors were added the next day. After 5 days of incubation, the cells were fixed with 4% paraformaldehyde and treated with PBS(-) containing 1% TritonX-100 and 1% bovine serum albumin. The

cells were then treated with anti-PA tag, Rat Monoclonal Antibody (1:1000, 4°C, overnight, Fujifilm Wako Pure Chemical Co.) and then with Goat Anti-Rat IgG H&L (Alexa Fluor® 488)(1:1000, rt, 1 h, Abcam Ltd.). The cells were covered with Prolong Gold antifade reagent with DAPI (Thermo Fisher Scientific Inc.) and observed under a fluorescence microscope.

Differentiation of preadipocytes with AAV or compound treatment

To differentiate 3T3-L1 cells, the medium was replaced with differentiation medium (growth medium containing 0.25 μM dexamethasone and 10 μg/mL insulin with or without 0.5 mM 3-isobutyl-1-methylxanthine (IBMX)) two days after the cells reached confluence (day 0). On day 2, the medium was replaced with growth medium or enhancer medium (growth medium with 5 μg/mL insulin). On day 4, the medium was replaced with growth medium.

To differentiate primary preadipocytes, the medium was replaced with differentiation medium (growth medium containing 0.5 mM IBMX, 5 μM dexamethasone, 1 μM rosiglitazone, and 10 μg/mL insulin) two days after reaching confluence (day 0). On day 3, the medium was replaced with growth medium or enhancer medium (growth medium with 10 μg/mL insulin). When the cells were maintained beyond day 6, the medium was replaced with the growth medium on days 6 and 9.

AAV vectors were added to the differentiation medium. Viral titers are described in the figure legends. For the knockdown experiments, T2 and T4 targeting vectors were used in combination. The same titers of empty vectors (for overexpression), scrambled vectors (for knockdown of *Tas2r108*), and negative control vector (for knockdown of *Tas2r126*) were added to the control cells.

T2R agonists and inhibitors were added on day 2. The compounds were dissolved in dimethyl sulfoxide (DMSO) and diluted with differentiation medium. The percentage of DMSO was kept below 0.5%, and the same concentration of DMSO was added to control cells.

After cell differentiation, lipid content was visualized and measured using the AdipoRed™ assay reagent (Lonza K.K., Tokyo, Japan).

Gene expression analysis

Total RNA was extracted using the FastGene™ RNA Basic Kit (Nippon Genetics Co., Ltd., Tokyo,

372 Japan), and cDNA was constructed using the ReverTra Ace qPCR RT Master Mix with gDNA Remover
373 (Toyobo Co., Ltd., Osaka, Japan).

374 Expression analysis of *Tas2r108* and *Tas2r126* was performed using the GeneAce Probe qPCR
375 Mix II (Nippon Gene Co., Ltd., Tokyo, Japan). The primer pairs and probes used are listed in Table 1. Gene
376 expression analysis of other genes was performed using the GeneAce SYBR™ qPCR Mix α (Nippon Gene
377 Co., Ltd., Tokyo, Japan). The primer pairs used are listed in Table 2. *Actb* was selected as a reference gene
378 by comparison with *Gapdh* and *Hprt1*.

379

380 Table 1. Primers and probes for T2R gene expression analysis

Gene name Acc. Num.	Sequence (5'-3')
Tas2r108	Forward: TGCAGAGAAACAGGACCAGC
NM_020502.1	Reverse: AGGAAGATAGAGCAGGGTAGCA
	Probe: FAM-CAGACGGAGGCTCACATGGGTGC-BHQ
Tas2r126	Forward: CTCACAGCAGAGCCCTGAAG
NM_207028.1	Reverse: CAGGGCCAATACCACACATTATC
	Probe: FAM-TGCGGTGTCCTTTGTGTCCATGA-BHQ
Actb	Forward: TACGACCAGAGGCATACAG
NM_007393.5	Reverse: GCCAACCGTGAAAAGATGAC
	Probe: FAM-TTGAGACCTTCAACACCCCAGCCA-BHQ

381

382 Table 2. Primer pairs for qPCR analysis

Gene name Acc. Num.	Sequence (5'-3')
Actb	Forward:TACGACCAGAGGCATACAG
NM_007393.5	Reverse:GCCAACCGTGAAAAGATGAC
Cebpa	Forward:GCAAAGCCAAGAAGTCGGTGGA
NM_007678.4	Reverse:CCTTCTGTTGCGTCTCCACGTT
Cebpb	Forward: TGATGCAATCCGGATCAA
NM_009883.4	Reverse: CACGTGTGTTGCGTCAGTC
Egr2	Forward: CCTTTGACCAGATGAACGGAGTG
NM_010118.3	Reverse: CTGGTTTCTAGGTGCAGAGATGG
Nr4a1	Forward: GTGCAGTCTGTGGTGACAATGC
NM_010444.3	Reverse: CAGGCAGATGTACTTGGCGCTT
Nr4a2	Forward: CCGCCGAAATCGTTGTCAGTAC
NM_013613.3	Reverse: TTCGGCTTCGAGGGTAAACGAC
Nr4a3	Forward: ACGCCGAAACCGATGTCAGTAC
NM_015743.4	Reverse: CTCCTGTTGTAGTGGGCTCTTTG
Pparg	Forward: GTACTGTCGGTTTCAGAAGTGCC
NM_001308354.2	Reverse: ATCTCCGCCAACAGCTTCTCCT

383

384 Intracellular cAMP concentrations

385 3T3-L1 cells were seeded in 48-well plates (5×10^4 cell/well). The next day, the cells were treated

with an AAV vector and cultured for 3 days. The medium was then changed to the growth medium containing 0.1 mM forskolin and 0.5 mM IBMX and stimulated for 1 h. The intracellular cAMP concentration was evaluated by cyclic AMP ELISA kit (Cayman Chemical Co.) according to the manufacturer's instructions.

Statistical analysis

Experiments were repeated at least twice (n = 3-6), and representative data are expressed as the mean ± standard error of the mean (SEM). Except for qPCR, data were analyzed using GraphPad Prism software (version 10), with the statistical methods indicated in figure legends. qPCR data were analyzed using the Bio-Rad CFX Maestro 2.3 software.

Competing Interests

The authors have no relevant financial or non-financial interests to disclose.

Author Contributions

E. Kato conceived and designed the research; E. Kato, S. Oshima, Y. Adachi, and R. Imai performed the research and acquired, analyzed, and interpreted the data. E. Kato wrote the draft paper, and all authors were involved in revising the manuscript.

Data Availability

The data that support the findings of this study are available in the Materials and Methods, Results, and/or Supplemental Material of this article.

Funding

This research was funded by JSPS KAKENHI, Grant numbers 23K05107.

References

1. Behrens M and Schaefer S (2025) Bitter taste receptors. Chem Senses 50. doi: 10.1093/chemse/bjaf064
2. Chupeerach C, Tapanee P, On-Nom N, Temviriyanukul P, Chantong B, Reeder N, A.

Adegoye G and Tolar-Peterson T (2021) The influence of TAS2R38 bitter taste gene polymorphisms on obesity risk in three racially diverse groups. BioMedicine 11:43–49. doi: 10.37796/2211-8039.1175

3. Turner A, Veysey M, Keely S, Scarlett CJ, Lucock M and Beckett EL (2021) Genetic Variation in the Bitter Receptors Responsible for Epicatechin Detection Are Associated with BMI in an Elderly Cohort. Nutrients 13:571–571. doi: 10.3390/nu13020571

4. Ortega FJ, Aguera Z, Sabater M, Moreno-Navarrete JM, Alonso-Ledesma I, Xifra G, Botas P, Delgado E, Jimenez-Murcia S, Fernandez-Garcia JC, Tinahones FJ, Banos RM, Botella C, de la Torre R, Fruhbeck G, Rodriguez A, Estivill X, Casanueva F, Ricart W, Fernandez-Aranda F and Fernandez-Real JM (2016) Genetic variations of the bitter taste receptor TAS2R38 are associated with obesity and impact on single immune traits. Mol Nutr Food Res 60:1673–83. doi: 10.1002/mnfr.201500804

5. Dotson CD, Zhang L, Xu H, Shin Y-K, Vigues S, Ott SH, Elson AET, Choi HJ, Shaw H, Egan JM, Mitchell BD, Li X, Steinle NI and Munger SD (2008) Bitter Taste Receptors Influence Glucose Homeostasis. PLoS ONE 3:e3974–e3974. doi: 10.1371/journal.pone.0003974

6. Kok BP, Galmozzi A, Littlejohn NK, Albert V, Godio C, Kim W, Kim SM, Bland JS, Grayson N, Fang M, Meyerhof W, Siuzdak G, Srinivasan S, Behrens M and Saez E (2018) Intestinal bitter taste receptor activation alters hormone secretion and imparts metabolic benefits. Molecular Metabolism 16:76–87. doi: 10.1016/j.molmet.2018.07.013

7. Niethammer AG, Zheng Z, Timmer A and Lee TL (2022) First-in-Human Evaluation of Oral Denatonium Acetate (ARD-101), a Potential Bitter Taste Receptor Agonist: A Randomized, Double-Blind, Placebo-Controlled Phase 1 Trial in Healthy Adults. Clin Pharmacol Drug Dev 11:997–1006. doi: 10.1002/cpdd.1100

8. Kimura S and Kato E (2020) TAS2R expression profile in brown adipose, white adipose, skeletal muscle, small intestine, liver and common cell lines derived from mice. Gene Reports 20:100763. doi: 10.1016/j.genrep.2020.100763

9. Cancello R, Micheletto G, Meta D, Lavagno R, Bevilacqua E, Panizzo V and Invitti C (2020) Expanding the role of bitter taste receptor in extra oral tissues: TAS2R38 is expressed in human adipocytes. Adipocyte 9:7–15. doi: 10.1080/21623945.2019.1709253

10. Peng H, Cheng Q, Chen J, Wang Y, Du M, Lin X, Zhao Q, Chen S, Zhang J and Wang X (2025) Green Tea Epigallocatechin-3-gallate Ameliorates Lipid Accumulation and Obesity-Associated Metabolic Syndrome via Regulating Autophagy and Lipolysis in Preadipocytes and Adipose Tissue. J Agric Food Chem 73:12272–12291. doi: 10.1021/acs.jafc.5c00973

11. Kimura S, Tsuruma A and Kato E (2022) Taste 2 Receptor Is Involved in Differentiation of 3T3-L1 Preadipocytes. Int J Mol Sci 23:8120. doi: 10.3390/ijms23158120

12. Ning X, He J, Shi XE and Yang G (2016) Regulation of Adipogenesis by Quinine through the ERK/S6 Pathway. International Journal of Molecular Sciences 17:504–504. doi: 10.3390/ijms17040504

13. Kohl S, Behrens M, Dunkel A, Hofmann T and Meyerhof W (2013) Amino Acids and Peptides Activate at Least Five Members of the Human Bitter Taste Receptor Family. Journal of Agricultural and Food Chemistry 61:53–60. doi: 10.1021/jf303146h

14. Farmer SR (2006) Transcriptional control of adipocyte formation. Cell Metab 4:263–73.

457 doi: 10.1016/j.cmet.2006.07.001
458 15. Chao LC, Bensinger SJ, Villanueva CJ, Wroblewski K and Tontonoz P (2008) Inhibition of
459 adipocyte differentiation by Nur77, Nurr1, and Nor1. Mol Endocrinol 22:2596–608. doi:
460 10.1210/me.2008-0161
461 16. Fang F, Ooka K, Bhattacharyya S, Wei J, Wu M, Du P, Lin S, Del Galdo F, Feghali-
462 Bostwick CA and Varga J (2011) The early growth response gene Egr2 (Alias Krox20) is a novel
463 transcriptional target of transforming growth factor-beta that is up-regulated in systemic sclerosis
464 and mediates profibrotic responses. Am J Pathol 178:2077–90. doi: 10.1016/j.ajpath.2011.01.035
465 17. Lossow K, Hubner S, Roudnitzky N, Slack JP, Pollastro F, Behrens M and Meyerhof W
466 (2016) Comprehensive Analysis of Mouse Bitter Taste Receptors Reveals Different Molecular
467 Receptive Ranges for Orthologous Receptors in Mice and Humans. J Biol Chem 291:15358–77. doi:
468 10.1074/jbc.M116.718544
469 18. Yan W, Sunavala G, Rosenzweig S, Dasso M, Brand JG and Spielman AI (2001) Bitter
470 taste transduced by PLC-beta(2)-dependent rise in IP(3) and alpha-gustducin-dependent fall in
471 cyclic nucleotides. Am J Physiol Cell Physiol 280:C742–51. doi: 10.1152/ajpcell.2001.280.4.C742
472 19. Caicedo A, Pereira E, Margolskee RF and Roper SD (2003) Role of the G-protein subunit
473 alpha-gustducin in taste cell responses to bitter stimuli. J Neurosci 23:9947–52. doi:
474 10.1523/JNEUROSCI.23-30-09947.2003
475 20. Guo L, Li X and Tang QQ (2015) Transcriptional regulation of adipocyte differentiation: a
476 central role for CCAAT/enhancer-binding protein (C/EBP) beta. J Biol Chem 290:755–61. doi:
477 10.1074/jbc.R114.619957
478 21. Fumoto T, Yamaguchi T, Hirose F and Osumi T (2007) Orphan nuclear receptor Nur77
479 accelerates the initial phase of adipocyte differentiation in 3T3-L1 cells by promoting mitotic clonal
480 expansion. J Biochem 141:181–92. doi: 10.1093/jb/mvm018
481 22. Li F, Wang D, Zhou Y, Zhou B, Yang Y, Chen H and Song J (2008) Protein kinase A
482 suppresses the differentiation of 3T3-L1 preadipocytes. Cell Res 18:311–23. doi: 10.1038/cr.2008.12
483 23. Fan L, Yang J, Shen C, Wu Z and Hu H (2021) Circ_0030586 inhibits cell proliferation and
484 stemness in bladder cancer by inactivating the ERK signaling via miR-665/NR4A3 axis. Acta
485 Histochem 123:151745. doi: 10.1016/j.acthis.2021.151745
486 24. Ashraf S, Hegazy YK and Harmancey R (2019) Nuclear receptor subfamily 4 group A
487 member 2 inhibits activation of ERK signaling and cell growth in response to beta-adrenergic
488 stimulation in adult rat cardiomyocytes. Am J Physiol Cell Physiol 317:C513–C524. doi:
489 10.1152/ajpcell.00526.2018
490 25. Schaefer S, Ziegler F, Lang T, Steuer A, Di Pizio A and Behrens M (2024) Membrane-bound
491 chemoreception of bitter bile acids and peptides is mediated by the same subset of bitter taste
492 receptors. Cell Mol Life Sci 81:217. doi: 10.1007/s00018-024-05202-6
493 26. Ziegler F, Steuer A, Di Pizio A and Behrens M (2023) Physiological activation of human
494 and mouse bitter taste receptors by bile acids. Commun Biol 6:612. doi: 10.1038/s42003-023-04971-
495 3
496 27. DeLuca JH and Reilly SM (2023) Culture and Differentiation of Primary Preadipocytes
497 from Mouse Subcutaneous White Adipose Tissue. Methods Mol Biol 2662:11–24. doi: 10.1007/978-
498 1-0716-3167-6_2

499 28. Silva JM, Li MZ, Chang K, Ge W, Golding MC, Rickles RJ, Siolas D, Hu G, Paddison PJ,
500 Schlabach MR, Sheth N, Bradshaw J, Burchard J, Kulkarni A, Cavet G, Sachidanandam R,
501 McCombie WR, Cleary MA, Elledge SJ and Hannon GJ (2005) Second-generation shRNA libraries
502 covering the mouse and human genomes. Nature Genetics 37:1281–1288. doi: 10.1038/ng1650
503 29. Negrini M, Wang G, Heuer A, Björklund T and Davidsson M (2020) AAV Production
504 Everywhere: A Simple, Fast, and Reliable Protocol for In-house AAV Vector Production Based on
505 Chloroform Extraction. Current Protocols in Neuroscience 93:1–10. doi: 10.1002/cpns.103
506

Supplementary data

Regulation of the murine preadipocytes differentiation by bitter taste receptor Tas2r108 and Tas2r126

Eisuke Kato,[a*] Shota Oshima,[b] Yusuke Adachi,[b] and Reitaro Imai[b]

[a] *Research Faculty of Agriculture, Hokkaido University, Sapporo, Japan;* [b] *Graduate School of Agriculture, Hokkaido University, Sapporo, Japan*

* Corresponding author
Eisuke Kato, e-mail: eikato@eis.hokudai.ac.jp

Contents

Supplementary Figures

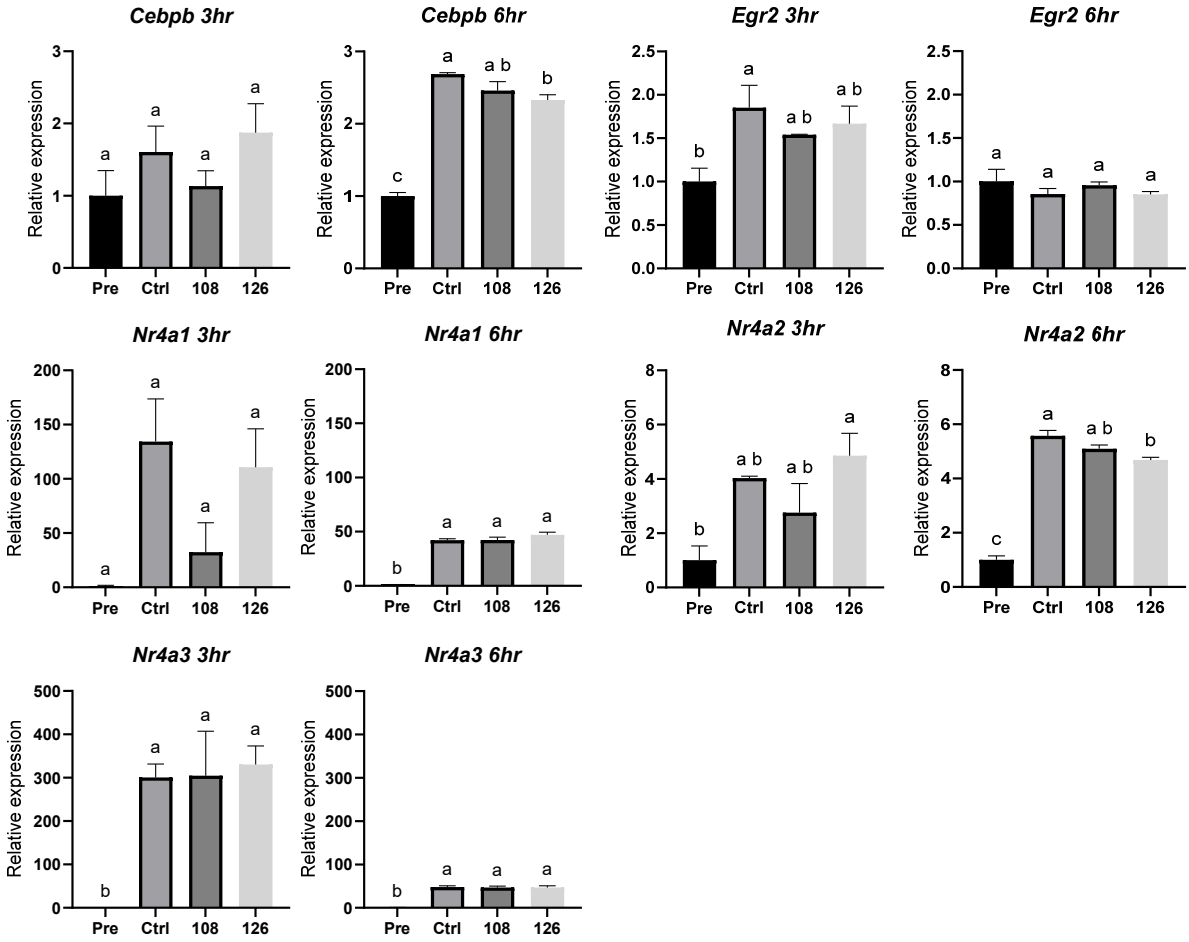

Figure S1. Gene expression of transcription factors in *Tas2r108* and *Tas2r126* overexpressed cells 3 and 6 hours after the start of differentiation induction.

3T3-L1 cells were seeded in 48 well plates and treated with an AAV vector (1×10^{10} vg/well) diluted in differentiation medium. Gene expression was assessed 3 or 6 hr after differentiation induction. Pre: pre-adipocytes, Ctrl: control cells treated with empty vector, 108/126: cells treated with Tas2r108 or Tas2r126 overexpression vector. Different letter indicates significant difference between the groups ($p<0.05$, Tukey's multiple comparisons test).

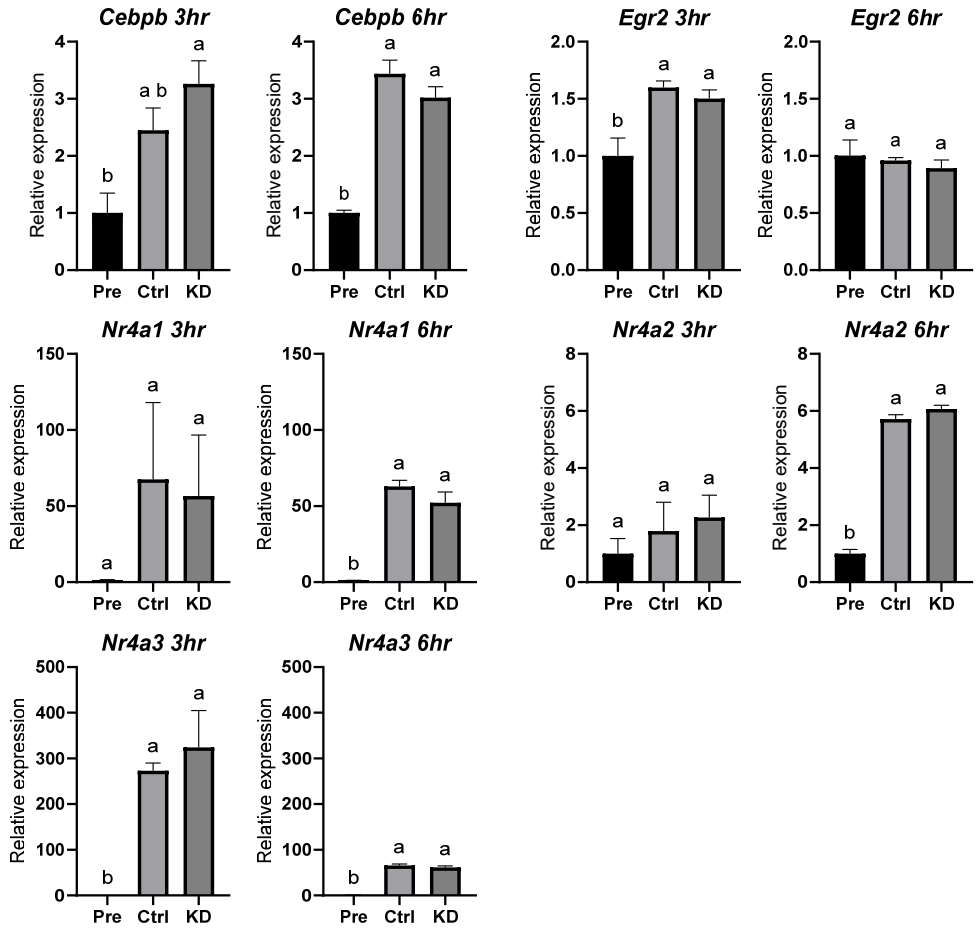

Figure S2. Gene expression of transcription factors in *Tas2r108* knockdown cells 3 and 6 hours after the start of differentiation induction.

3T3-L1 cells were seeded in 48 well plates and treated with an AAV vector (KD: 5×10^9 vg/well) diluted in differentiation medium. Gene expression was assessed 3 or 6 hr after differentiation induction. Pre: pre-adipocytes, Ctrl: control cells treated with scrambled vector, KD: cells treated with Tas2r108 KD vector. Different letter indicates significant difference between the groups ($p<0.05$, Tukey's multiple comparisons test).

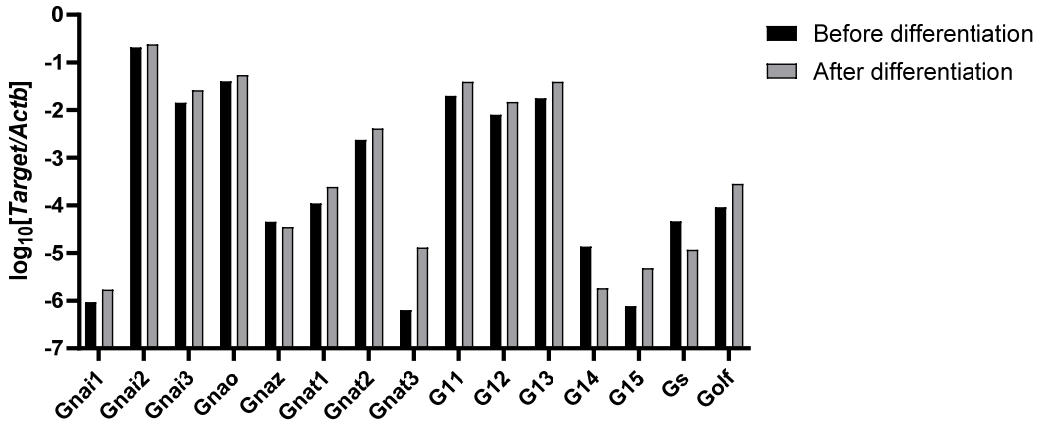

Figure S3. Gene expression level of G-protein in 3T3-L1 cells.
Primer pairs are listed in Table S1.

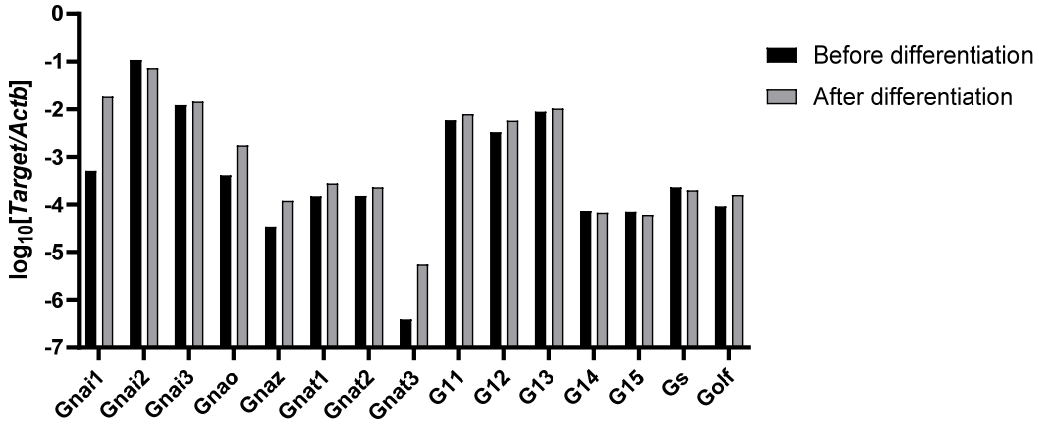

Figure S4. Gene expression level of G-protein in mouse primary cells.
Primer pairs are listed in Table S1.

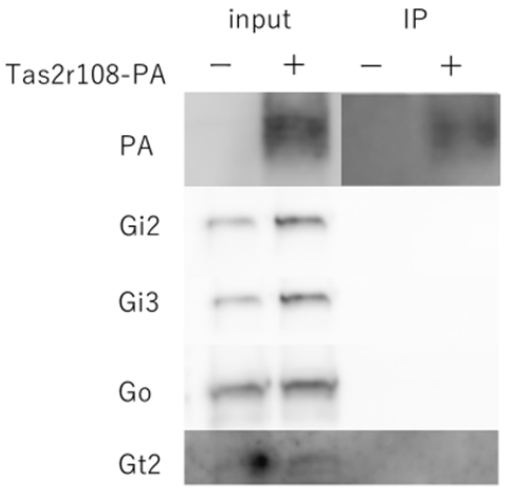

Figure S5. Co-immunoprecipitation (IP) analysis.

PA-tagged Tas2r108 were expressed in 3T3-L1 cells using AAV. The extracted protein was immunoprecipitated using anti-PA tag antibody and analyzed by western blotting.

- Figure S7

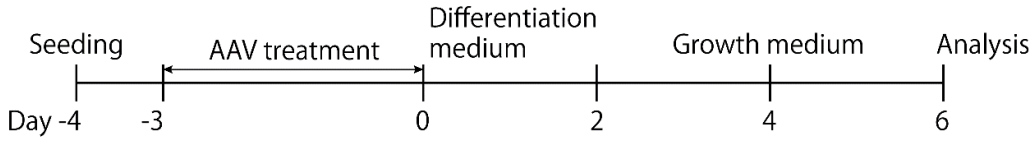

- Figure 2-4

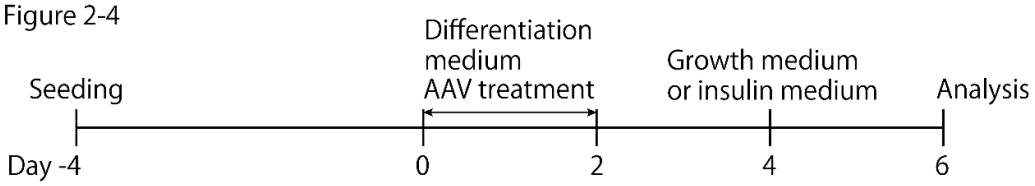

Figure S6. Schedule for AAV treatment and differentiation of 3T3-L1 cells

.

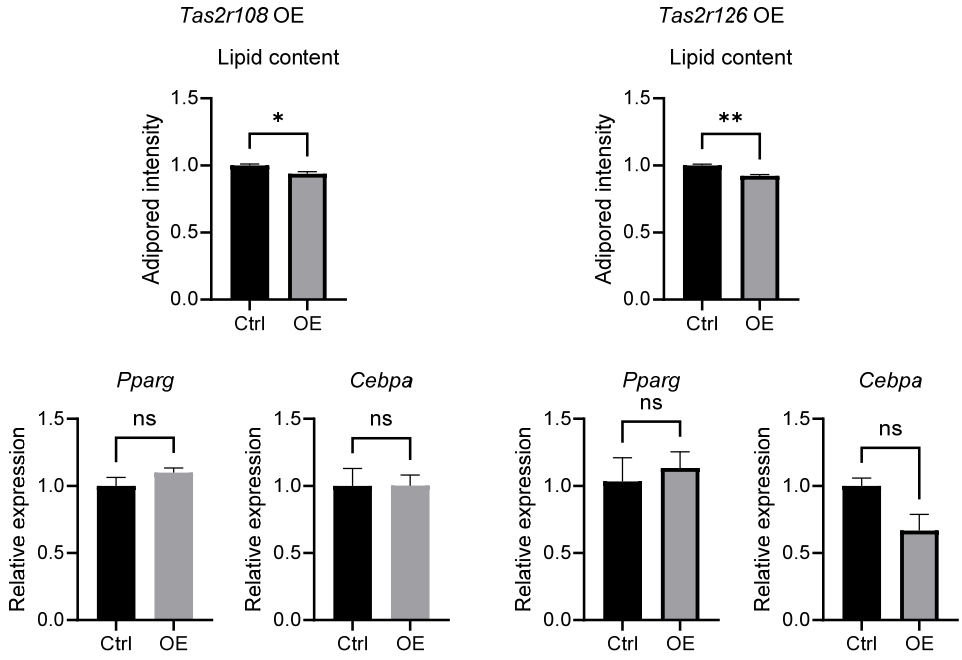

Figure S7. *Tas2r108* and *Tas2r126* overexpression prior to differentiation has weak effect on the lipid content of 3T3-L1 cells.

3T3-L1 cells were seeded in 48 well plate and treated with an AAV vector (1×10^{10} vg/well) for 3 days. Then the cells were induced for differentiation with IBMX, dexamethasone, and insulin. The cells were cultured until day 6 in growth medium. ns: no significance, *P<0.05, **P<0.01 (t-test).

Supplementary Table

Table S1. Primer pairs

Target gene	Sequence
Actb	Forward : CATTGCTGACAGGATGCAGAAGG
	Reverse : TGCTGGAAGGTGGACAGTGAGG
Gnai1	Forward : CTTCTGTGTGGCCCTGAGTGA
	Reverse : GATGGACGTGTCTGTAAACCACTTG
Gnai2	Forward : ACAACAAGTGGTTCACAGACACCTC
	Reverse : TAGCTGGCTGCCTCGTCGTA
Gnai3	Forward : TGAAGACTACAGGCATTGTGGAGAC
	Reverse : GTTCGGATCTTTGGCCACCTA
Gnao	Forward : TGGTCTACAGCAACACCATCCAG
	Reverse : TTCCATACGACTCACCACGTCA
Gnaz	Forward : CAGTGGCTATGACCTGAAGCTC
	Reverse : GGAAGAGGATGAGCGAGGTGTT
Gnat1	Forward : AACCGAATGCACGAGAGCCT
	Reverse : AGAGCCCGCAGTCTTTGAGG
Gnat2	Forward : AATCGCATGCACGAGTCTTTG
	Reverse : AGAGCCCACAGTCCTTGAGG
Gnat3	Forward : CACCTCCATTGTTCTGTTTCTTAAC
	Reverse : GCATCTTCAAATGTGTTTGGTC
Gna11	Forward : GTTCTTGGTGGCACTAAGCGAG
	Reverse : GACAGACGAGTTCTGGAACCAG
Gna12	Forward : TCCACCTTCCTCAAGCAGATGC
	Reverse : AGCGTCCACAAGAACCCTCGAA
Gna13	Forward : TCCACCTTCCTGAAGCAGATGC
	Reverse : AGCTTCTCTCGGGCATCTACCA
Gna14	Forward : TGACCAGGTTCTGGCTGAGTGT
	Reverse : ACGGAGGAGTTCAGAAACCAGG
Gna15	Forward : GTGATTGCCCTCATCTACCTGG
	Reverse : ATGACCGAGGTGCTCTTGAACC
Gnas	Forward : CCATTGAGATGCGAGAGCAGAAG
	Reverse : GGTGCTTTTGCCAGACTCTCCA
Gnal	Forward : ACACCAGATGCGGGAGAAGATC
	Reverse : CTGCGGATGTTCTCTGTGTCCA

Methods

Immunoprecipitation

3T3-L1 cells were seeded at a concentration of 2×10^5 cells/well into a 12-well plate. The following day, AAV1-Tas2r108 was added at a concentration of 8×10^{11} vg/well and the cells were cultured for 5 days. After washing with PBS(-), 200 µL/well of NP-40 buffer (25 mM Tris, 150 mM NaCl, 1 mM EDTA, 1% NP-40, pH 7.4) containing protease and phosphatase inhibitors was added and the cells were lysed. The lysate was centrifuged at 5,000 g at 4°C, and the supernatant was collected.

The lysate was loaded to the anti-PA-tag antibody beads, incubated for 2 hours at 4°C. The beads were washed four times with NP-40 buffer and the absorbed proteins were recovered with the addition of 50 µL of 2 mg/mL PA-tag peptide in TBS (25 mM Tris, 150 mM NaCl, pH 7.4). After 30 min incubation at 4°C, the supernatant was collected, separated by SDS-PAGE and transferred to PVDF membrane. The lysate was also separated as the input protein.

The membrane was blocked by 5% non-fat dry milk in TBS-T for 1 hr and then incubated with 1st antibody at 4°C for overnight. The membrane was incubated in the 2nd antibody for 1 hr at room temperature and detected by either ImmunoStar LD, ImmunoStar Zeta (Fujifilm Wako Pure Chemical Co.), or EzWestLumi One (Atto Co.). Following antibody and dilutions were used.

1st antibody

PA: Anti PA-tag antibody, 1:2000 (Fujifilm Wako Pure Chemical Co., 016-25861)

Gi2: GNAI2 Polyclonal antibody, 1:2000 (Proteintech Group Inc., 11136-1-AP)

Gi3: GNAI3 Polyclonal antibody, 1:5000 (Proteintech Group Inc., 11641-1-AP)

Go: GNAO1 Polyclonal antibody, 1:2000 (Proteintech Group Inc., 12635-1-AP)

Gt2: GNAT2 antibody, 1:2000 (GeneTex, GTX134342)

2nd antibody

HRP-conjugated Goat Anti-Rat IgG(H+L), 1:2000 (Proteintech Group Inc., SA00001-15)

Anti-rabbit IgG, HRP-linked Antibody, 1:2000 (Cell Signaling Technology, 7074S)

Additional data

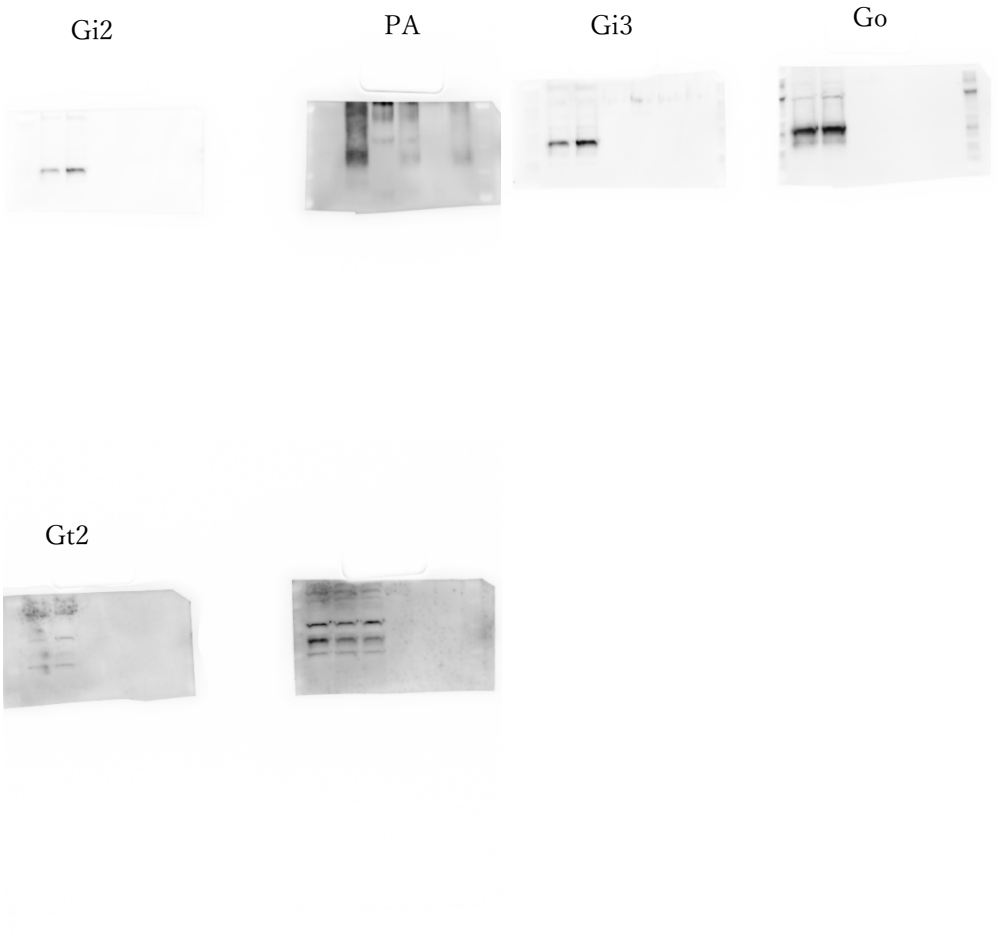

Uncropped images of western blotting data.